Intestinal Epithelial Ablation of Pit-2/Slc20a2 in Mice Leads to Sustained Elevation of Vitamin D 3 Upon Dietary Restriction of Phosphate

Pastor-Arroyo, Eva Maria ; Knöpfel, Thomas ; Imenez Silva, Pedro Henrique ; Schnitzbauer, Udo ; Poncet, Nadège ; Biber, Jürg ; Wagner, Carsten A ; Hernando, Nati

Abstract: AIM Several Na^+ -dependent phosphate cotransporters namely NaPi-IIb/SLC34A3, Pit-1/SLC20A1 and Pit-2/SLC20A2, are expressed at the apical membrane of enterocytes but their contribution to active absorption of phosphate is unclear. The aim of this study was to compare their pattern of mRNA expression along the small and large intestine and to analyse the effect of intestinal depletion of Pit-2 on phosphate homeostasis. METHODS Intestinal epithelial Pit-2 deficient mice were generated by crossing floxed Pit-2 with villin-Cre mice. Mice were fed two weeks standard or low phosphate diets. Stool, urine, plasma and intestinal and renal tissue were collected. Concentration of electrolytes and hormones, expression of mRNAs and proteins and intestinal transport of tracers were analysed. RESULTS Intestinal mRNA expression of NaPi-IIb and Pit-1 is segment-specific whereas the abundance of Pit-2 mRNA is comparable along the whole intestine. In ileum, NaPi-IIb mRNA expression is restricted to enterocytes whereas Pit-2 mRNA is found in epithelial and non-epithelial cells. Overall, their mRNA is not regulated by dietary phosphate. The absence of Pit-2 from intestinal epithelial cells does not affect systemic phosphate-homeostasis under normal dietary conditions. However, in response to dietary phosphate restriction, Pit-2 deficient mice showed exacerbated hypercalciuria and sustained elevation of $1,25(OH)_2$ vitamin D_3 . CONCLUSIONS In mice, the intestinal Na^+ /phosphate cotransporters are not coexpressed in all segments. NaPi-IIb but not Pit-2 mRNA is restricted to epithelial cells. Intestinal epithelial Pit-2 does not contribute significantly to absorption of phosphate under normal dietary conditions. However, it may play a more significant role upon dietary phosphate restriction.

DOI: https://doi.org/10.1111/apha.13526

PROFESSOR CARSTEN A. WAGNER (Orcid ID : 0000-0002-9874-8898)
DR NATI HERNANDO (Orcid ID : 0000-0002-1692-0544)

Article type : Regular Paper

Intestinal epithelial ablation of Pit-2/Slc20a2 in mice leads to sustained elevation of vitamin D_3 upon dietary restriction of phosphate

Short title: Phosphate balance in the absence of Pit-2 in intestine

Eva Maria Pastor-Arroyo, Thomas Knöpfel, Pedro Henrique Imenez Silva, Udo Schnitzbauer, Nadège Poncet, Jürg Biber, Carsten A. Wagner* and Nati Hernando*

University of Zürich, Institute of Physiology - Zürich, Switzerland

* Both authors contributed equally to this work

Corresponding author:
Carsten A. Wagner and Nati Hernando
Institute of Physiology
University of Zurich
Winterthurerstrasse 190
CH-8057 Zurich
Switzerland
Email: wagnerca@access.uzh.ch; hernando@physiol.uzh.ch
Phone: +41-44-6355054
Fax: +41-44-6356814

This article has been accepted for publication and undergone full peer review but has not been through the copyediting, typesetting, pagination and proofreading process, which may lead to differences between this version and the Version of Record. Please cite this article as doi: 10.1111/APHA.13526

Abstract

Aim Several Na^+-dependent phosphate cotransporters namely NaPi-IIb/SLC34A3, Pit-1/SLC20A1 and Pit-2/SLC20A2, are expressed at the apical membrane of enterocytes but their contribution to active absorption of phosphate is unclear. The aim of this study was to compare their pattern of mRNA expression along the small and large intestine and to analyse the effect of intestinal depletion of Pit-2 on phosphate homeostasis.

Methods Intestinal epithelial Pit-2 deficient mice were generated by crossing floxed Pit-2 with villin-Cre mice. Mice were fed two weeks standard or low phosphate diets. Stool, urine, plasma and intestinal and renal tissue were collected. Concentration of electrolytes and hormones, expression of mRNAs and proteins and intestinal transport of tracers were analysed.

Results Intestinal mRNA expression of NaPi-IIb and Pit-1 is segment-specific whereas the abundance of Pit-2 mRNA is comparable along the whole intestine. In ileum, NaPi-IIb mRNA expression is restricted to enterocytes whereas Pit-2 mRNA is found in epithelial and non-epithelial cells. Overall, their mRNA is not regulated by dietary phosphate. The absence of Pit-2 from intestinal epithelial cells does not affect systemic phosphate-homeostasis under normal dietary conditions. However, in response to dietary phosphate restriction, Pit-2 deficient mice showed exacerbated hypercalciuria and sustained elevation of $1,25(OH)_2$vitamin D_3.

Conclusions In mice, the intestinal Na^+/phosphate cotransporters are not coexpressed in all segments. NaPi-IIb but not Pit-2 mRNA is restricted to epithelial cells. Intestinal epithelial Pit-2 does not contribute significantly to absorption of phosphate under normal dietary conditions. However, it may play a more significant role upon dietary phosphate restriction.

Key words:

Intestinal absorption, phosphate, Slc20, Slc34, vitamin D_3,

Introduction

The small intestine expresses several Na^+-dependent phosphate (Pi) cotransporters at the apical membrane of enterocytes that are potentially involved in active transport of Pi across the intestinal epithelia. These transporters belong to the SLC20 and SLC34 families of solute carriers, with the SLC20 family consisting of 2 members (Pit-1/SLC20A1 and Pit-2/SLC20A2) whereas 3 cotransporters constitute the SLC34 branch (NaPi-IIa/SLC34A1, NaPi-IIb/SLC34A2 and NaPi-IIc/SLC34A3) (for review see[1]). Pit-1, Pit-2 and NaPi-IIb have been localized to the brush border membrane (BBM) of enterocytes and therefore have the potential to mediate uptake of dietary Pi from the gut lumen[2,3]. Although current data suggests that NaPi-IIb plays a major quantitative role[4,5], the presence of additional transporters has been proposed based on the finding that transport activity and expression of known cotransporters do not always change in parallel[6]. In addition to the active mode, a passive paracellular component most probably contributes to intestinal absorption of Pi[7-12].

The expression of intestinal Na^+/Pi cotransporters is sensitive to dietary Pi content and to 1,25 $(OH)_2$ vitamin D_3 (1,25$(OH)_2D_3$) status. Transport activity and cotransporters protein abundance are reduced in response to chronic feeding on high Pi, while upregulation is observed in response to chronically administered low Pi[3,6,13-17]. However, the time required for adaptation varies between 1 day and 5 days[6] . Thus, changes in NaPi-IIb and Pit-2 are detected already 24 hours after dietary switches; instead, regulation of Pit-1 protein abundance responds to chronic (5 -10 days) but not acute dietary changes. On the other hand, a raise in plasma levels of 1,25$(OH)_2D_3$ leads to higher NaPi-IIb protein abundance[13]. The levels of 1,25$(OH)_2D_3$ increase in response to dietary Pi deprivation; however, this change is not required for dietary regulation of NaPi-IIb, as the cotransporter properly adapts to the content of Pi in the chow even when 1,25$(OH)_2D_3$ signalling is disrupted[14,15]. The effect of 1,25$(OH)_2D_3$ on Pit transporters has not been analysed.

The distribution of NaPi-IIb along the intestinal axis is species-specific. In mice, NaPi-IIb is enriched in the ileum[16], whereas the proximal segments of the small intestine show the highest levels in rats[3,17]. Intestinal ablation of NaPi-IIb in mice abrogates Na^+/Pi cotransport in ileum but has a minor effect on Pi homeostasis under normal dietary conditions[4,5]. However when maximally expressed (i.e upon feeding on low Pi), NaPi-IIb contributes to up to 50% of intestinal Pi absorption[4]. In agreement with this large contribution, maintenance of normophosphatemia in Pi-deprived NaPi-IIb$^{-/-}$ mice requires mobilization of skeletal Pi[18].

Pit-1 and Pit-2 were originally identified as membrane receptors for gibbon ape leukaemia virus (Glvr-1)[19] and murine amphotropic retrovirus (Ram-1)[20] respectively, though their function as Na^+/Pi cotransporters was soon recognized[20,21]. Both SLC20 cotransporters have affinities for Na^+ (50 mM) and Pi (100 μM) in the same range as those displayed by NaPi-IIb but, unlike the SLC34 members, Pit transporters transport preferentially monovalent ($H_2PO_4^-$) instead of divalent (HPO_4^{2-}) Pi[22]. Both SLC20 transporters are ubiquitously expressed[23], and are accordingly involved in a variety of processes. Pit-2 participates in Pi-induced calcification of vascular smooth muscle cells[24], it is required for Pi-induced secretion of FGF23[25] and contributes to the clearance of Pi from the cerebrospinal fluid[26]. In this regard, mutations in *SLC20A2* are linked to familial idiopathic basal ganglia calcification (FIBGC: OMIM 213600)[26]. Recently, both SLC20 members were proposed to play a role in sensing of extracellular Pi, a function that would not require their transport activity[27]. Also recently it was reported that postnatally-induced depletion of Pit-1 and Pit-2 from skeletal muscle results in failure to drive and early mortality probably secondary to myofiber necrosis/myopathy caused by increased energy-stress and reduced generation of ATP in muscles[28]. The intestinal pattern of expression of Pit-1 and Pit-2 has been studied only in rats. In this model, Pit-1 mRNA levels increase progressively from the duodenum to the ileum, though the higher protein expression is detected in jejunum, with lower levels in duodenum and absent from ileum[3]. In contrast, Pit-2 mRNA abundance seems to be homogenous along the entire rat small intestine[3]. The expression of these transporters in the large intestine has not been analysed. Similarly, the contribution of intestinal Pits to systemic Pi balance has not been investigated.

Here, we report the pattern of expression of NaPi-IIb, Pit-1 and Pit-2 mRNAs along the small and large intestine of mice and the effect of intestinal depletion of Pit-2 on Pi homeostasis under standard and low dietary Pi.

Results

Generation of intestinal Pit-2/*Slc20a2* deficient mice

The Na^+/Pi cotransporter Pit-2 is a transmembrane protein of about 650 amino acids. *Slc20a2*, the gene encoding Pit-2, consist of 11 exons with the codon for the initiator methionine located in exon 2 and the stop codon in exon 11 (supplementary Fig. 1a). The loxed-exon 4 contains 89 bp and encodes for amino acids 144-172. The presence of the loxed-gene in the first generation of pups upon morula aggregation and implantation was analyzed by PCR using two different combinations of primers (supplementary Fig. 1a-b). One combination (Slc20a2-for + loxR) is expected to produce an amplicon of 328 bp in the mutated gene, and no amplification in wild types since the antisense primer overlaps with the 3' loxP site, whereas the second combination (Slc20a2-5'arm + LAR3 + Slc20a2-3'arm) should result in 246 and 410 bp fragments in loxed and wild type DNA, respectively. As shown in supplementary Fig. 1b several heterozygous and one wild type pup were born from one of the foster mothers. Upon breeding with Flp full deleters for excision of the β-gal/neo cassettes (supplementary Fig. 1c), the second combination of primers produced the 410 bp fragment in wild type DNA and an amplicon >500 bp in mutated DNA (data not shown). For the depletion of *Slc20a2* from the intestinal epithelia, upon excision of the β-gal/neo cassette floxed mice were further mated with villin-Cre mice, a transgenic line in which the expression of Cre-recombinase is under the control of the villin promoter[29,30]. Their offspring was genotyped by PCR using the Slc20a2-5'arm + Slc20a2-3'arm primers (amplicons of 410 bp in wild type DNA and >500 bp in mutated DNA) as well as with CRE3 + CRE4 primers to detect the presence of the Cre-recombinase (supplementary Fig. 1c-d). Cre-mediated removal of exon 4 is expected to result in a frame shift introducing a stop codon about 340 bp downstream. Therefore, *Slc20a2* deficient mice should express an mRNA encoding a truncated protein of 258 residues of which only the first 144 correspond to the cotransporter sequence and the last 114 are unrelated.

***Slc20* and *Slc34* transporters have different patterns of intestinal mRNA expression**

The abundance of each transporter mRNA was simultaneously quantified in all 5 intestinal segments from wild type (+/+) and Pit-2 deficient mice (f/f) fed standard diet. As shown in Fig. 1a, the expression of Pit-1/*Slc20a1* mRNA in +/+ animals was similar in duodenum, jejunum, ileum and proximal colon, whereas its abundance in the distal colon was significantly higher than in all other segments. The pattern of expression of Pit-2/*Slc20a2* mRNA in +/+ mice was similar to that of Pit-1, with higher expression in distal colon than in the rest of the segments, though the differences was not as pronounced as for Pit-1 (Fig. 1b). As expected based on previous reports[16,17], the expression of NaPi-IIb/*Slc34a2* mRNA along the small

intestine of +/+ mice was higher in the ileum and barely detectable in duodenum (Fig. 1c). Furthermore, only low levels were observed in colon, with comparable expression in proximal and distal segments.

Incubation of ileum slides from +/+ mice with *in situ* hybridization probes for Pit-2/*Slc20a2* mRNA resulted in sparse but clear positive signal in the form of dots (Fig. 1d, d'). Dots were observed though out the whole intestinal tissue, including muscle wall, villi and crypts. Within the villi, dots were found in the lining epithelial cells and in the interstitium of villi. Of note, due to the small size of the floxed exon (89 bp), the Pit-2 probes for conventional RNAscope do not allow the discrimination between +/+ and f/f RNA. Hybridization with NaPi-IIb/*Slc34a2* mRNA probes resulted in stronger signal (Fig. 1e, e'). NaPi-IIb mRNA was detected as highly abundant red dots exclusively located in epithelial cells lining the villi, whereas the interstitium of villi, crypts and the muscle cells were negative. As expected, incubation of intestinal tissue with probes for the mouse peptidyl-prolyl cis-trans isomerase B (*Ppib*) as positive control resulted in abundant red dots enriched in the epithelia (both villi and crypts) but also present in the interstitium of villi and the muscle wall (Fig. 1f). In contrast, no signal was detected with probes for the bacterial dihydrodipicolinate reductase (*DapB*) as negative control probes (Fig. 1g).

Complementing the *in situ* hybridization data with immunohistochemistry was hampered by the lack of an antibody recognizing the cotransporter in mouse tissue. An antibody raised in rabbit against rat Pit-2 that has been thoroughly characterized in rat samples[6,31] failed to detect the cotransporter in sections from jejunum prepared from wild type mice as well as in OK cells transfected with a plasmid encoding mouse Pit-2 fused to the myc epitope (supplementary Fig. 2). Although incubation with a commercial antibody raised in mouse stained cells within the interstitium of villi, the same signal was detected only with the secondary antibody (supplementary Fig. 3). Both antibodies detected bands at around 70 kDa in homogenates from jejunum (supplementary Fig. 4) and kidney (supplementary Fig. 5). However, these bands were not upregulated in homogenates of wild type mice fed with low Pi, unlike what has been described in rats, suggesting that either they detect Pit-2 unrelated proteins or that the expression of the cotransporter in mice is too low to be detected with these antibodies.

Villin-driven Cre-recombinase depletes the intestinal epithelia from Pit-2/*Slc20a2* mRNA without altering the expression of Pit-1 and NaPi-IIb

Villin-driven Cre recombinase has been shown to specifically drive Cre-mediated recombination in the gut epithelia[29], and we reported previously that breeding NaPi-IIb-floxed mice with villin-driven Cre transgenic results in efficient ablation of NaPi-IIb from the ileum epithelia[5]. Because unlike NaPi-IIb, Pit-2/*Slc20a2* mRNA is equally distributed along the small and large intestine, we first analyzed the intestinal expression

of villin by qPCR. The gene was expressed in all five segments, though the abundance in colon was smaller than in the small intestine (villin/HPRT relative expressions: 14.53 ± 2.76 in duodenum, 19.68 ± 1.90 in jejunum, 16.25 ± 2.28 in ileum, 1.33 ± 0.15 in proximal colon and 1.80 ± 0.11 in distal colon). Villin-driven Cre-recombinase led to a strong reduction of Pit-2/*Slc20a2* mRNA (more than 95%) along the whole intestine of f/f mice (Fig 1b).

The absence of Pit-2 did not alter the expression of either Pit-1/*Slc20a1* (Fig. 1a) or NaPi-IIb/*Slc34a2* (Fig. 1c) transcripts in the intestinal epithelia, except for a reduction in the expression of Pit-1 in the distal colon. Furthermore, the abundance of the NaPi-IIb protein in homogenates from ileum mucosa was also similar in both genotypes (Fig. 2a), with NaPi-IIb/actin ratios of 1.50 ± 0.23 and 2.11 ± 0.29 arbitrary units in +/+ and f/f mice, respectively.

Depletion of intestinal epithelial Pit-2/*Slc20a2* does not reduce the incorporation of ^{32}P into jejunal BBMV or the paracellular transport of ^{32}P

Uptakes of ^{32}P were analyzed in BBMV isolated from jejunum (Fig. 2b). This segment was chosen to avoid maximal expression of NaPi-IIb (ileum) while still containing enough epithelial tissue to process material from single mice. Uptake experiments were carried out in the presence of 0.1 mM cold substrate, a concentration that supports Pi transport mediated by Slc34 as well Slc20 transporters. Reactions were performed at pH 7.4, a condition in which both monovalent ($H_2PO_4^-$) and divalent Pi ions (HPO_4^{2-}) are present, as well as at pH 6, where the monovalent ion is the major form. At both pH values, BBMV were incubated in the presence/absence of Na^+ (to discriminate between Na^+-dependent and Na^+-independent mechanisms), with or without PFA in the Na^+-media (to distinguish between Slc34- and Slc20-mediated incorporation, since at the used concentration PFA should only inhibit Slc34 transporters). The total uptake of ^{32}P into jejunal BBMV from +/+ mice was higher at pH 6 than at pH 7.4 (Fig. 2b, white bars) and PFA inhibited uptake at both pH values. Further, at both pH values, the Na^+-independent component was very small (about 5% of the total uptake). Depletion of Pit-2 had no effect on the Pi-transport activity of jejunal BBM (Fig. 2b, blue bars), with all transport components having similar values in f/f and +/+ samples.

Paracellular transport of ^{32}P across duodenum, jejunum, ileum and distal colon was analyzed in Ussing chambers. As we reported recently[12], incubation of intestinal segments in the presence of 70 mM Pi on the apical side and no Pi added on the basolateral side resulted in a time-dependent recovery of ^{32}P from the basolateral chamber that remained linear within 2 hours after initiation (supplementary Fig. 6). Average flux rates (nmol/mm^2/h) were calculated as the mean of fluxes measured at 3 time points (60, 90 and 120 minutes). As shown in Fig. 2c, flux rates were comparable in duodenum, jejunum and distal

colon, whereas ileum showed a higher rate. However, the fluxes in all segments were similar in tissues from +/+ and f/f mice, suggesting that intestinal depletion of Pit-2 does not affect the paracellular permeability for Pi.

Depletion of intestinal epithelial Pit-2/*Slc20a2* does not affect Pi levels but leads to hypercalciuria upon chronic restriction of dietary Pi

The fecal, urinary and plasma levels of Pi and Ca^{++} were measured simultaneously in samples from +/+ and f/f mice kept either on the standard diet or fed a low Pi diet for 14 days. Similar amounts of Pi were measured in feces from +/+ and f/f mice under standard diet (Fig. 3a). Furthermore, both genotypes reduced to a similar extent their fecal output when challenged with low Pi. The urinary excretion of Pi was similar in +/+ and f/f mice fed standard chow and both genotypes showed comparable reductions in urinary Pi output in response to dietary Pi restriction (Fig. 3b). No differences in plasma Pi were detected either between genotypes or between dietary protocols (Fig. 3c). The fecal excretion of Ca^{++} was similar in +/+ and f/f mice, with both genotypes reducing the fecal output when fed on low Pi chow (Fig. 3d). The urinary excretion of Ca^{++} was also comparable in +/+ and f/f mice fed standard diet (Fig. 3e). As expected, hypercalciuria developed upon two weeks dietary Pi restriction and this effect was significantly more pronounced in f/f than +/+ mice. The concentration of Ca^{++} in plasma was not influenced by the dietary Pi content and was similar in both genotypes under both dietary conditions (Fig. 3f).

Depletion of intestinal epithelial Pit-2/*Slc20a2* does not alter the mRNA abundance of intestinal Slc20 and Slc34a2 upon chronic restriction of dietary Pi

The relative abundance of each transporter mRNA in a particular intestinal segment was simultaneously quantified in samples from all four groups of mice (supplementary Fig. 7). For each intestinal segment and gene, the expression on mice fed low Pi was normalized to their corresponding abundance in mice of the same genotype fed standard dietary Pi. The intestinal expression of Pit-1/*Slc20a1* mRNA was not regulated by dietary Pi neither in +/+ nor in f/f mice (Fig. 4a). mRNA abundance of Pit-2/*Slc20a2* in +/+ mice (and its residual expression in f/f mice) was also insensitive to dietary Pi except in the ileum, where the expression in Pi restricted +/+ mice was about twice as high as in +/+ mice fed on standard diet (Fig. 4b). Although the relative abundance of NaPi-IIb/*Slc34a2* mRNA tended to be reduced in the small intestine of mice fed on low Pi (Fig. 4c), this was due to a large scatter of values in the groups fed on standard chow, resulting in high mean expression, rather than an actual reduction in the groups deprived of Pi (see supplementary Fig. 2). Dietary Pi did not alter the expression of NaPi-IIb/*Slc34a2* mRNA in the large intestine (Fig. 4c). The abundance of NaPi-IIb at the protein level was also similar in BBM from ileum

of +/+ and f/f mice fed on low Pi (Fig. 4d), with NaPi-IIb/actin ratios of 0.90 ± 0.15 and 0.74 ± 0.11 arbitrary units respectively.

Depletion of intestinal epithelial Pit-2/*Slc20a2* does not alter plasma levels of PTH and intact FGF-23 and renal abundance of Slc34 Na^+/Pi transporters

As shown in Fig. 5a, +/+ and f/f mice had similar PTH values when fed standard diet. Furthermore, PTH was properly and similarly reduced in both genotypes upon feeding on low Pi. Intact FGF-23 levels were also similar in +/+ and f/f mice under both dietary conditions, with the groups fed on low Pi having the expected hormonal reduction (Fig. 5b). Although the concentration of intact FGF-23 tended to be lower in f/f mice fed low Pi than in their +/+ littermates, the difference did not reach statistical significance.

The expression of the renal cotransporters NaPi-IIa and NaPi-IIc was similar in BBM of +/+ and f/f mice, both under standard and Pi restricted diets (Fig. 5c). As expected, the abundance of both cotransporters was increased in +/+ mice upon feeding low Pi, and a similar change was observed in f/f animals. On the other hand, the renal mRNA expression of Pit-2 was similar in both genotypes and dietary conditions (Fig. 5d). Likewise, the mRNA expression of Pit-2 (Fig. 5e) and Pit-1 (Fig. 5f) in bones was comparable in all four groups.

Depletion of intestinal epithelial Pit-2/*Slc20a2* associates with higher 1,25$(OH)_2$ vitamin D_3 upon chronic restriction of dietary Pi

Plasma levels of 1,25$(OH)_2D_3$ were similar in +/+ and f/f mice fed standard diet (Fig. 6a). 1,25$(OH)_2D_3$ values were also comparable in +/+ mice fed normal or low Pi. In contrast, f/f mice subjected to dietary Pi restriction had 1,25$(OH)_2D_3$ levels twice as high as those fed with standard chow (Fig. 6a). The expression of renal *Cyp27b1* mRNA was similar in +/+ and f/f mice fed standard diet, as well as in +/+ mice fed standard and low Pi diets (Fig. 6b). Although a tendency for higher expression of the activating hydroxylase was observed in f/f mice fed on low Pi, the difference did not reach statistical significance due to the large data scatter (Fig. 6b). The mRNA expression of *Cyp24a1* was also similar in kidneys from +/+ and f/f mice fed standard diets (Fig. 6c), and its abundance was reduced in mice fed on low Pi, with the difference being significant in +/+ animals. However, quantification of Cyp24a1 at the protein level indicated similar abundance in renal homogenates of all four groups of mice (Fig. 6d). The renal expression of the vitamin D receptor (VDR) at the mRNA (Fig. 6e) and protein levels (Fig. 6d) was also similar in +/+ and f/f mice both under standard and low dietary Pi. The renal protein expression of the Ca^{2+} channel Trpv5 and the Ca^{2+}-binding protein calbindin D28k were comparable in both genotypes and dietary conditions (Fig. 7a, b). The urinary excretion of DPD, a urinary marker for bone resorption, was also similar in all four groups of mice (Fig. 7c).

Discussion

Several Na^+-dependent Pi cotransporters, namely NaPi-IIb, Pit-1 and Pit-2, are expressed in intestinal epithelial cells and are proposed to contribute to the active absorption of dietary Pi. While the role of NaPi-IIb has been experimentally demonstrated[5], the potential contribution of the Slc20 orthologues has not been analysed in detail. The intestinal protein abundance of Pit-1 and Pit-2 in rats respond to the content of Pi in the diet, but only Pit-2 expression is regulated in the short term (1 day) whereas changes in Pit-1 take much longer (5 to 10 days depending on the intestinal segment). Furthermore, regulation of Pit-2 expression at the BBM of rat renal proximal tubules is also under the control or dietary Pi[31] (and PTH[32]), suggesting that this cotransporter may play a role in transepithelial transport of Pi. Here we have compared the mRNA pattern of expression of NaPi-IIb, Pit-1 and Pit-2 along the intestine of mice and investigated the contribution of intestinal epithelial Pit-2 to overall Pi absorption in this murine model.

We reproduced the previously reported pattern of expression of NaPi-IIb mRNA along the small intestine[16,17], i.e higher expression in ileum and lower in duodenum, and additionally we observed low and similar expression of this transporter in proximal and distal colon. In agreement with the known protein expression[13], NaPi-IIb mRNA abundance is restricted to enterocytes. Low and comparable levels of Pit-1 mRNA were detected along the small intestine and proximal colon, whereas the transporter is enriched in distal colon. This observation is in contrast with the pattern of expression reported in rats, where Pit-1 was shown to increase progressively from the duodenum to the ileum[3], suggesting that, as NaPi-IIb, the intestinal pattern of expression of Pit-1 is species-specific. Our findings also indicate a potential heterogeneity of the colonic epithelia with regard to Pi handling, a feature already suggested at functional level. Thus, recently published *in vitro* (everted sleeves) and *in vivo* experiments (*in situ* ligated intestinal loops) indicate that the proximal colon of rats has only low levels of Pi transport activity, and that this activity shows features of passive transport including its dependence on the luminal Pi concentration even in the mM range and its Na^+-independence[33]. Instead, the distal colon displays a large capacity to transport Pi, with transport values comparable to those of the duodenal mucosa, though whether or not this distal transport is Na^+-dependent remains unanswered since *in vitro* and *in vivo* approaches provided contradictory data[33]. In contrast to Pit-1 and NaPi-IIb, the expression of Pit-2 was similar along the whole intestine, an observation that is in agreement with previous reports showing comparable levels of Pit-2 mRNA along the small intestine of rats[3]. Moreover, *in situ* hybridization indicates that unlike NaPi-IIb, intestinal Pit-2 mRNA is expressed in epithelial and non-epithelial cells. Though it does not rule out specific roles, this finding is consistent with the originally proposed

housekeeping function of Pit-2. For all three cotransporters, dietary Pi does not seem a main transcriptional regulator.

In agreement with previous findings[6,34,35], the total uptake of ^{32}P into jejunal BBMV from +/+ mice was higher at pH 6 than at pH 7.4, suggesting a larger contribution of transporters preferring monovalent Pi as substrate (Pit transporters). However, and in line with previous data generated in rats[6], PFA was able to inhibit uptakes at both pH, pointing to a role of NaPi-IIb even at pH 6 or to the presence of another, yet unknown, Na^+-dependent Pi transporter. In fact, based on this apparent contradiction, the contribution of additional transporters to active intestinal transport of Pi was postulated[6]. Regardless of whether or not other transporters are involved in handling of Pi in the gut, depletion of Pit-2 from the intestinal epithelia did not alter uptake of Pi into jejunal BBMV. Pit-2 deficient mice were able to maintain phosphate balance without compensatory upregulation of NaPi-IIb or Pit-1, suggesting that Pit-2 does not contribute significantly to active intestinal absorption of Pi in mice under normal dietary conditions. Also paracellular fluxes of Pi were not altered in the absence of Pit-2 possibly explaining maintenance of normophosphatemia under these conditions. In agreement, fecal, urinary and plasma concentration of Pi as well as Pi-regulating hormones (PTH, FGF23 and $1,25(OH)_2D_3$) and renal Na^+-dependent Pi cotransporters (NaPi-IIa and NaPi-IIc) were indistinguishable in +/+ and f/f mice fed standard diet. These observations are in agreement with a previous report showing that constitutive and global ablation of Pit-2 does not modify neither urinary and plasma Pi nor PTH and FGF23 levels in mice fed standard diets[25].

Challenge with low dietary Pi for 2 weeks triggered similar compensatory adaptations in fecal and urinary excretion of Pi in +/+ and f/f mice, such that despite the reduced intake of Pi both groups remained normophosphatemic. We have already reported that wild type and intestinal-specific NaPi-IIb deficient mice retained/restored normophosphatemia after 14 days under low dietary Pi, a response that in wild type seemed to depend solely on higher renal reabsorption, though increased bone resorption may also be required in NaPi-IIb depleted mice[18]. Similar to the work presented here, no differences in serum or urinary Pi were reported between wild type mice and mice with full ablation of Pit-2 after one week of low (0.05%), normal (0.55%) or high Pi (1.65%) diets, except for a reduction in serum Pi in mutant mice fed on high Pi compared with wild types[25]. In our model, the compensatory reduction in urinary excretion of Pi in response to low dietary Pi reflects upregulation of NaPi-IIa and NaPi-IIc, the Slc34 cotransporters expressed in renal proximal tubules that are responsible for reabsorption of Pi from the primary urine (for review see[36]). In turn, upregulation of NaPi-IIa and NaPi-IIc is the renal response to lower plasma levels of PTH and FGF23, two phosphaturic hormones synthetized by the parathyroid gland and osteocytes/osteoblast, respectively, in response to high plasma Pi[31,32,37-40]. Reductions in phosphaturia and

plasma PTH/FGF23 as well as upregulation of NaPi-IIa/NaPi-IIc were comparable in both genotypes fed on low Pi. In contrast to our data, while comparable reductions in phosphaturia and plasma PTH were also reported in mice with full depletion of Pit-2 and their wild type counterparts fed low Pi, FGF23 failed to adapt in mutant mice[25]. Using isolated bone shafts, the authors showed that Pit-2 is required for proper secretion of FGF23 in response to high Pi media and the same group recently proposed that both Pit-1 and Pit-2 mediate Pi-sensing independently of their transport activity[27]. Since in our model the expression of Pit-2 and Pit-1 in bones is normal, the response of FGF-23 to dietary Pi is preserved.

Unlike the above parameters, the hypercalciuric response to low dietary Pi was exacerbated in our f/f mice, an effect associated with higher $1,25(OH)_2D_3$ levels. $1,25(OH)_2D_3$ is an steroid hormone whose last activation step takes place in renal proximal cells and is stimulated in response to hypophosphatemia[41]. In the small intestine, $1,25(OH)_2D_3$ promotes absorption of Pi by upregulating the expression of NaPi-IIb[13]. The observation that $1,25(OH)_2D_3$ levels were similar in +/+ mice fed standard and low Pi diets is in agreement with previous reports showing that the increase of $1,25(OH)_2D_3$ triggered by low dietary Pi is transient, with higher values detected three days after dietary restriction and normalizing thereafter[18]. However, in the absence of intestinal epithelial Pit-2, $1,25(OH)_2D_3$ remains high even after two weeks feeding on low Pi. Although we could not identify the mechanism responsible (either increased synthesis/Cyp27b1 and/or reduced catabolism/Cyp24a1), this finding indicates that in the absence of Pit-2 in enterocytes, mice depend upon sustained elevation of $1,25(OH)_2D_3$ to maintain normophosphatemia when challenged with low dietary Pi. Because $1,25(OH)_2D_3$ also stimulates intestinal absorption of Ca^{2+}, the excess of the Ca^{2+} must then be excreted with the urine. While we could not find upregulation of Trpv5 or calbindin D28k, the intestinal origin of the hypercalciuric response (as opposed to bone resorption) is supported by the similar urinary excretion of DPD, a marker for osteoclastic activity, observed in all groups of mice. Of note, no differences in urinary excretion of Ca^{2+} were found between wild type and full constitutive Pit-2 deficient mice fed on low Pi, though both groups showed hypercalciuria compared with mice fed on normal Pi diets[25]. Whether this discrepancy between both models is related to the different adaptation of FGF-23 mentioned above is not known, and $1,25(OH)_2D_3$ had not been reported.

In summary, we have shown that the intestinal expression of Pit-1/Slc20a1, Pit-2/Slc20a2 and NaPi-IIb/Slc34a2 mRNAs in mice is segment specific and is not regulated by chronic restriction of dietary Pi. NaPi-IIb mRNA expression is restricted to epithelial cells whereas Pit-2 mRNA is expressed both in epithelial and non-epithelial cells. Intestinal epithelial-specific depletion of Pit-2 does not alter fecal or urinary excretion of Pi neither under standard nor under low dietary Pi. However, it results in exacerbated hypercalciuria, probably secondary to higher $1,25(OH)_2D_3$ levels, in mice challenged with low dietary Pi, suggesting a more sustained activation of $1,25(OH)_2D_3$ production in the absence of Pit-2.

Material and Methods

Generation of intestinal-specific Pit-2/*Slc20a2* knockout mice

Embryonic stem (ES) cells transfected with a *Slc20a2* targeting vector were purchased from the International Knockout Mouse Consortium (IKMC)/ European Conditional Mouse Mutagenesis Program (EUCOMM). After homologous recombination of the targeting vector in the ES cells, exon 4 was flanked by *loxP* sites (supplementary Fig. 1a). Upstream of the 5' *loxP* site, the vector contained a cassette for production of β-galactosidase (β-gal) followed by a neomycin phosphotransferase gene (neo cassette). ES cells were sent to the Institute of Labortierkunde (LTK) of the University of Zurich for morula aggregation and implantation into foster mothers. The presence of the targeting vector in newborns was analyzed by two sets of PCR amplification of genomic DNA. The first PCR set was done in the presence of a forward primer annealing to exon 4 (Slc20a2-for) and a reverse primer annealing to the 3' *loxP* site (LoxR). The second set was performed with a forward primer designed in intron 3-4 upstream of the β-gal and neo cassettes (Slc20a2-5'arm) and two reverse oligos, one annealing within the β-gal sequence (LAR3) and the second one in intron 3-4 downstream of the neo cassette (Slc20a2-3'arm) (supplementary Fig. 1a-b). Upon breeding to homozygosity, loxed/loxed mice were cross with Flp full deleters (64Flp3B6) for removal of β-gal/neo cassettes (supplementary Fig. 1c). After confirmation of removal, floxed pups were bred with villin-driven Cre transgenic mice for ablation of Pit-2/*Slc20a2* in intestinal epithelia (Fig. 1c)[29,30]. Genotyping of pups born from this last breeding was performed by PCR using the Slc20a2-5'arm and Slc20a2-3'arm primers, with expected amplicons of 410 and >500 base pairs for wild type and floxed DNA, respectively (supplementary Fig. 1d). The sequences of genotyping primers are indicated in Table 1 and their locations in the targeting vector are shown in supplementary Fig. 1a, c. Primer sequences and PCR protocol were provided by IKMC. All genotyping reactions were performed using as template genomic DNA isolated from ear punches.

Animal handling and collection of samples

Animal handling was approved by the local veterinary authority (Kantonales Veterinäramt Zürich), and complied with Swiss Animal Welfare laws. Studies were performed with 10-14 weeks old wild type (floxed mice, villin-Cre negative) and intestinal-depleted *Slc20a2* male littermates, housed with standard 12 hours dark-light cycles and free access to food and water. Mice were fed during the last 14 days with either standard diet (0.8% Pi, 1% Ca^{++} and 1000 IU/kg vitamin D_3; KLIBA ≠ 2169) or with low Pi containing chow (0.1% Pi, 1% Ca^{++} and 1000 IU/kg vitamin D_3; KLIBA ≠ 3436). Upon 3 days of gradual adaptation to individual metabolic cages (Tecniplast, Italy), stool and urine were collected during the last 24 hours. On the last day, mice were anaesthetized (isoflurane) and venous blood was withdrawn in heparinized

syringes; samples were immediately centrifuged (7000 x g, for 7 minutes at 4°C) and plasma aliquoted. The whole intestine was dissected, rinsed with cold PBS and everted for collection of mucosal scrapings from duodenum, jejunum, ileum, proximal colon and distal colon. Plasma, intestinal mucosa, kidneys and femurs were immediately snap-frozen in liquid nitrogen and stored at -80°C until further use. Urine was centrifuged at room temperature (10000 x g, for 10 min) to remove debris, and supernatants were store at -20°C. Stool was dried at 65°C for 24 hours and also stored at 20°C.

Quantification of mRNA expression by real time PCR

After extraction of total RNA from intestinal mucosa, renal tissue and bones (RNAeasy Minikit, Qiagen), cDNA was synthetized by standard methods (TaqMan Reverse Transcription Kit, Applied Biosystems) and used as template for real time PCR. PCR amplification was performed by adding specific pairs of forward (Fw) and reverse (Rv) primers and FAM/TAMRA-labelled probes (Pb) to a commercially available reaction mix (TaqMan Universal PCR Master Mix). The Fw primer for Pit-2/*Slc20a2* quantification anneals in exon 3, whereas the Rv primer anneals in exon 4 and the probe spans both exons. The expression of tested genes was normalized to the abundance of either HPRT or 18S (commercial primers and probe purchased from Mycrosynth) according to the formula $R = 2^{[Ct(\text{control gene})-Ct(\text{test gene})]}$, where R is the relative ratio and Ct indicates the cycle number at a given threshold. Sequences of primers and probes are shown in Table 1.

mRNA *in situ* hybridization

"Swiss rolls" were prepared from ileum of wild type mice as reported[42]. In brief, segments were open up longitudinally, fixed in 4% paraformaldehyde (PFA)/PBS for 1 hour at 4°C, rolled up longitudinally and further fixed in 4% PFA overnight at 4°C. Upon sequential incubation in 15% (2 hours at 4°C) and 30% sucrose/PBS (overnight at 4°C), samples were embedded in Optimal Cutting Temperature medium (Cell Path) prior freezing on dry ice. Tissue sections of about 5 μm were prepared with a cryotome (Leica Biosystems), mounted on Superfrost slides (Thermo Fisher Scientific) and processed for *in situ* hybridization using the RNAscope 2.5HD chromogenic assay (Bio-techne) according to the manufacturer's recommendations. In brief, upon rehydration in PBS and target retrieval, tissue samples were hybridized for 2 hours at 40°C with either *Slc20a2* or *Slc34a2* mRNA probes. Additional samples were incubated with probes for the bacterial dihydrodipicolinate reductase (*DapB*) and the mouse peptidyl-prolyl cis-trans isomerase B (*Ppib*) as negative and positive controls, respectively. Upon hybridization, sections were process for signal amplification followed by incubation with alkaline phosphatase-labelled probes. Upon incubation with Fast Red substrate and counterstaining with Gill's Hematoxylin I, sections were mounted with VectaMount Mounting Medium HT-5000 (Vector Laboratories, Burlingame, CA, USA). Chromogenic signal was analyzed with a Leica DM 55008 microscope.

Immunofluorescence of intestine from wild type mice and myc-Pit-2 transfected OK cells

Cryosections of jejunum and ileum from wild type mice were processed for immunofluorescence with either a polyclonal antibody against rat Pit-2[6] (a gift Dr. Moshe Levi and Dr Victor Sorribas; dilution 1: 100) or a monoclonal antibody against the mouse cotransporter (purchased from Santa Cruz: ≠ sc-377326; dilution 1: 100). Primary antibodies were incubated over night at 4°C. The appropriate anti-rabbit/mouse secondary antibodies (Alexa Fluor 594; Life Technologies) were mixed with Alexa Fluor 488-coupled phalloidin (Life Technologies) and with 4,6-diamidino-2-phenylindole (DAPI; Sigma), for the detection of actin and nuclei respectively. Immunostainings were performed either in untreated samples or in samples subjected to two antigen retrieval protocols prior addition of primary antibodies: preincubation in either 1% SDS/PBS for 5 minutes at room temperature or in 0.3% triton/PBS for 15 minutes at room temperature. Upon mounting (DAKO), samples were analyzed with a Leica DM 55008 fluorescence microscope.

Opossum kidney cells (OK cells; clone 3B/2) were incubated in DMEM/Ham's F-12 medium (1:1) supplemented with 10% fetal calf serum, 2 mM glutamine and 20 mM Hepes. Cells were plated on coverslips in 12-multiwell dishes (TPP) and upon reaching about 70% confluence were transfected overnight in the presence of Lipofectamine 2000 (Invitrogen) with a plasmid coding for the mouse Pit-2 fused C-terminally to the myc-DDK epitope (OriGene MR224161). After reaching confluence cells were permeabilized with 0.1% saponin/PBS for 30 minutes and co-incubated for 2 hours with the polyclonal Pit-2 antibody (1: 100) and a monoclonal anti-myc antibody (Invitrogen). DAPI (Sigma) was added together with secondary antibodies (Alexa Fluor 488-anti rabbit and Alexa Fluor 594-anti mouse; Life Technologies) and incubated for 30 minutes. All incubations were done at room temperature. Coverslips were finally mounted and cells were analyzed on a Leica DM 55008 fluorescence microscope.

Quantification of Pi and Ca^{++} in stool, urine and plasma

The concentration of Pi in stool, urine and plasma was measured according to the Fiske Subbarow method (Randox, United Kingdom), and a QuantiChrom assay kit (Bio-Assay Systems) was used to quantify the concentration of Ca^{++}. Urinary creatinine was determined by the Jaffe method (Wako Chemicals).

Quantification of PTH, FGF23 and $1,25(OH)_2D_3$ in plasma and of DPD in urine

The concentrations of intact parathyroid hormone (PTH) and intact fibroblast growth factor 23 (FGF23) were measured using ELISA-based kits (Immunotopics), whereas the levels of VD_3 were quantified by radioimmunoassay (Immunodiagnostic System). Urinary deoxypyridinoline (DPD) was measured with an enzymatic immunoassay kit (Quidel Corporation, Athens, USA).

Uptake of radiolabeled Pi into intestinal BBMV and Ussing chambers fluxes

BBM vesicles (BBMV) were prepared from frozen duodenal mucosa using the Mg^{++} precipitation technique[43]. These vesicles were resuspended in a buffer (300 mM mannitol, 10 mM HEPES) adjusted at either pH 6 or pH 7.4 with 2-(*N*-morpholino)-ethanesulfonic acid or Tris respectively, as reported[6]. Uptakes of ^{32}P were performed according to the filtration technique as described in detail[44]. In brief, freshly isolated BBMV were incubated at 25°C in uptake solutions consisting of resuspension buffers (pH 6 and pH 7.4) containing 0.1 mM $PO_4H_2K/^{32}P$ and either 100 mM NaCl or 100 mM KCl. Additionally, 5 mM phosphonoformic acid (PFA) was added to the Na^+-containing solution. Uptakes were performed for 30 seconds and after termination, the incorporation of ^{32}P into the BBMV was quantified in a β-counter (Packard BioScience) and normalized to the protein concentration (Bio-Rad).

^{32}P fluxes across duodenum, jejunum, ileum and distal colon were measured in Ussing chambers equipped with a bubble lift system as described[12]. Ringer solutions were buffered at pH 6, and an apical-to-basolateral Pi gradient of 70 mM was stablished by adding on the apical side Ringer containing 70 mM NaH_2PO_4 and in the basolateral side a modified solution in which NaH_2PO_4 was replaced by $NaCl/NaHCO_3$. Upon addition of ^{32}P to the apical chamber, aliquots from the basolateral side were collected at 60, 90 and 240 minutes; aliquots of the same volume were also taken from the apical side to avoid changes in hydrostatic pressure. For the time 0, aliquots were taken just immediately prior addition of radiolabelled substrate. ^{32}P-phosphate transported to the acceptor side of the tissue was quantified using a β-counter (Packard BioScience).

Western blots

Westernblots of intestinal or renal samples (BBM or homogenates containing 20-40 μg of proteins) were done with primary antibodies against rat Pit-2 (a gift from Dr. M. Levi and Dr. Victor Sorribas; 1: 1000)[6], mouse Pit-2 (Santa Cruz:≠ sc-377326; 1: 500), NaPi-IIa (1: 3,000)[45], NaPi-IIb (1: 3,000)[2], NaPi-IIc (1: 3,000)[46], Trpv5 (a gift from Dr. O. Bonny, Lausanne-Switzerland; 1: 1,000)[47], VDR (Santa Cruz: ≠ sc-13133; 1: 500), Cbd28K (Swant: ≠ 300; 1: 2,000), Cyp24a1 (Proteintech: ≠ 21582-1-AP; 1: 1,000), β-actin (Sigma: ≠ A5316; 1: 10,000) and tubulin (Sigma: ≠ T4026; 1:20,000), following standard procedures. Upon 5 minutes exposure to HRP-substrate (Millipore), chemiluminescence signals were recorded with a luminescent image analyzer (LAS-4000, Fujifilm). Quantification was performed using ImageJ.

Statistical analysis

Differences between groups were analyzed by t-test (two groups) or ANOVA/ Bonferroni's test (multiple groups). $P < 0.05$ was considered significant. Data are shown as mean ± SEM.

All material submitted is conform with good publication practice in physiology 2019. Acta physiologica (Oxford, England), 227: e13405, 2019

Acknowledgments

The Swiss National Science Foundation (grant 31003A-176125 to C.A.W) supported this study. The polyclonal Pit-2 antibody raised in rabbits against the rat cotransporter was a gift from Dr. M. Levi (Georgetown University, Washington, DC, USA) and Dr. V. Sorribas (University of Zaragoza, Spain). Dr. Bonny, University of Lausanne, kindly provided anti-Trpv5 antibodies.

Conflict of interest

None

Data available on request from the authors

References

1. Forster IC, Hernando N, Biber J, Murer H. Phosphate transporters of the SLC20 and SLC34 families. *Mol Aspects Med.* 2013;34(2-3):386-395.
2. Hilfiker H, Hattenhauer O, Traebert M, Forster I, Murer H, Biber J. Characterization of a murine type II sodium-phosphate cotransporter expressed in mammalian small intestine. *Proc Natl Acad Sci U S A.* 1998;95(24):14564-14569.
3. Giral H, Caldas Y, Sutherland E, et al. Regulation of rat intestinal Na-dependent phosphate transporters by dietary phosphate. *Am J Physiol Renal Physiol.* 2009;297(5):F1466-1475.
4. Sabbagh Y, O'Brien SP, Song W, et al. Intestinal npt2b plays a major role in phosphate absorption and homeostasis. *J Am Soc Nephrol.* 2009;20(11):2348-2358.
5. Hernando N, Myakala K, Simona F, et al. Intestinal Depletion of NaPi-IIb/Slc34a2 in Mice: Renal and Hormonal Adaptation. *J Bone Miner Res.* 2015;30(10):1925-1937.
6. Candeal E, Caldas YA, Guillen N, Levi M, Sorribas V. Intestinal phosphate absorption is mediated by multiple transport systems in rats. *Am J Physiol-Gastr L.* 2017;312(4):G355-G366.
7. Mc HG, Parsons DS. The absorption of water and salt from the small intestine of the rat. *Q J Exp Physiol Cogn Med Sci.* 1957;42(1):33-48.
8. Walling MW. Intestinal Ca and Phosphate Transport - Differential Responses to Vitamin-D3 Metabolites. *Am J Physiol.* 1977;233(6):E488-E494.
9. Walton J, Gray TK. Absorption of Inorganic-Phosphate in the Human Small-Intestine. *Clin Sci.* 1979;56(5):407-412.
10. Danisi G, Straub RW. Unidirectional Influx of Phosphate across the Mucosal Membrane of Rabbit Small-Intestine. *Pflug Arch Eur J Phy.* 1980;385(2):117-122.
11. Hu MS, Kayne LH, Jamgotchian N, Ward HJ, Lee DBN. Paracellular phosphate absorption in rat colon: A mechanism for enema-induced hyperphosphatemia. *Miner Electrol Metab.* 1997;23(1):7-12.
12. Knoepfel T, Himmerkus N, Guenzel D, Bleich M, Hernando N, Wagner CA. Paracellular transport of phosphate along the intestine. *Am J Physiol-Gastr L.* 2019;317(2):G233-G241.
13. Hattenhauer O, Traebert M, Murer H, Biber J. Regulation of small intestinal Na-P-i type IIb cotransporter by dietary phosphate intake. *Am J Physiol-Gastr L.* 1999;277(4):G756-G762.
14. Segawa H, I K, Yamanaka S, et al. Intestinal Na-P(i) cotransporter adaptation to dietary P(i) content in vitamin D receptor null mice. *Am J Physiol-Renal.* 2004;287(1):F39-F47.

15. Capuano P, Radanovic T, Wagner CA, et al. Intestinal and renal adaptation to a low-Pi diet of type II NaPi cotransporters in vitamin D receptor- and 1alphaOHase-deficient mice. *Am J Physiol Cell Physiol.* 2005;288(2):C429-434.
16. Radanovic T, Wagner CA, Murer H, Biber J. Regulation of intestinal phosphate transport - I. Segmental expression and adaptation to low-P-i diet of the type IIb Na+-P-i cotransporter in mouse small intestine. *Am J Physiol-Gastr L.* 2005;288(3):G496-G500.
17. Marks J, Srai SK, Biber J, Murer H, Unwin RJ, Debnam ES. Intestinal phosphate absorption and the effect of vitamin D: a comparison of rats with mice. *Exp Physiol.* 2006;91(3):531-537.
18. Knopfel T, Pastor-Arroyo EM, Schnitzbauer U, et al. The intestinal phosphate transporter NaPi-IIb (Slc34a2) is required to protect bone during dietary phosphate restriction. *Sci Rep-Uk.* 2017;7.
19. Vanzeijl M, Johann SV, Closs E, et al. A Human Amphotropic Retrovirus Receptor Is a 2nd Member of the Gibbon Ape Leukemia-Virus Receptor Family. *P Natl Acad Sci USA.* 1994;91(3):1168-1172.
20. Kavanaugh MP, Miller DG, Zhang WB, et al. Cell-Surface Receptors for Gibbon Ape Leukemia-Virus and Amphotropic Murine Retrovirus Are Inducible Sodium-Dependent Phosphate Symporters. *P Natl Acad Sci USA.* 1994;91(15):7071-7075.
21. Olah Z, Lehel C, Anderson WB, Eiden MV, Wilson CA. The Cellular Receptor for Gibbon Ape Leukemia-Virus Is a Novel High-Affinity Sodium-Dependent Phosphate Transporter. *J Biol Chem.* 1994;269(41):25426-25431.
22. Ravera S, Virkki LV, Murer H, Forster IC. Deciphering PiT transport kinetics and substrate specificity using electrophysiology and flux measurements. *Am J Physiol-Cell Ph.* 2007;293(2):C606-C620.
23. Nishimura M, Naito S. Tissue-specific mRNA expression profiles of human solute carrier transporter superfamilies. *Drug Metab Pharmacok.* 2008;23(1):22-44.
24. Crouthamel MH, Lau WL, Leaf EM, et al. Sodium-Dependent Phosphate Cotransporters and Phosphate-Induced Calcification of Vascular Smooth Muscle Cells Redundant Roles for PiT-1 and PiT-2. *Arterioscl Throm Vas.* 2013;33(11):2625-2632.
25. Bon N, Frangi G, Sourice S, Guicheux J, Beck-Cormier S, Beck L. Phosphate-dependent FGF23 secretion is modulated by PiT2/Slc20a2. *Mol Metab.* 2018;11:197-204.
26. Wang C, Li YL, Shi L, et al. Mutations in SLC20A2 link familial idiopathic basal ganglia calcification with phosphate homeostasis. *Nat Genet.* 2012;44(3):254-256.
27. Bon N, Couasnay G, Bourgine A, et al. Phosphate (Pi)-regulated heterodimerization of the high-affinity sodium-dependent Pi transporters PiT1/Slc20a1 and PiT2/Slc20a2 underlies extracellular Pi sensing independently of Pi uptake. *J Biol Chem.* 2018;293(6):2102-2114.

28. Chande S, Caballero D, Ho BB, et al. Slc20a1/Pit1 and Slc20a2/Pit2 are essential for normal skeletal myofiber function and survival. *Sci Rep.* 2020;10(1):3069.
29. El Marjou F, Janssen KP, Chang BHJ, et al. Tissue-specific and inducible Cre-mediated recombination in the gut epithelium. *Genesis.* 2004;39(3):186-193.
30. Pinto D, Robine S, Jaisser F, El Marjou F, Louvard D. Regulatory sequences of the mouse villin gene that efficiently drive transgenic expression in immature and differentiated epithelial cells of small and large intestines. *J Biol Chem.* 1999;274(10):6476-6482.
31. Villa-Bellosta R, Ravera S, Sorribas V, et al. The Na+-Pi cotransporter PiT-2 (SLC20A2) is expressed in the apical membrane of rat renal proximal tubules and regulated by dietary Pi. *Am J Physiol Renal Physiol.* 2009;296(4):F691-699.
32. Picard N, Capuano P, Stange G, et al. Acute parathyroid hormone differentially regulates renal brush border membrane phosphate cotransporters. *Pflug Arch Eur J Phy.* 2010;460(3):677-687.
33. Marks J, Lee GJ, Nadaraja SP, Debnam ES, Unwin RJ. Experimental and regional variations in Na+-dependent and Na+-independent phosphate transport along the rat small intestine and colon. *Physiol Rep.* 2015;3(1).
34. Berner W, Kinne R, Murer H. Transport of Inorganic-Phosphate into Brush-Border Membrane-Vesicles Isolated from Rat Small-Intestine. *H-S Z Physiol Chem.* 1976;357(3):250-251.
35. Danisi G, Murer H, Straub RW. Effect of Ph on Phosphate-Transport into Intestinal Brush-Border Membrane-Vesicles. *Am J Physiol.* 1984;246(2):G180-G186.
36. Levi M, Gratton E, Forster IC, et al. Mechanisms of phosphate transport. *Nat Rev Nephrol.* 2019;15(8):482-500.
37. Centeno PP, Herberger A, Mun HC, et al. Phosphate acts directly on the calcium-sensing receptor to stimulate parathyroid hormone secretion. *Nat Commun.* 2019;10.
38. Perwad F, Azam N, Zhang MYH, Yamashita T, Tenenhouse HS, Portale AA. Dietary and serum phosphorus regulate fibroblast growth factor 23 expression and 1,25-dihydroxyvitamin D metabolism in mice. *Endocrinology.* 2005;146(12):5358-5364.
39. Pfister MF, Ruf I, Stange G, et al. Parathyroid hormone leads to the lysosomal degradation of the renal type II Na/P-i cotransporter. *P Natl Acad Sci USA.* 1998;95(4):1909-1914.
40. Weinman EJ, Steplock D, Shenolikar S, Biswas R. Fibroblast Growth Factor-23-mediated Inhibition of Renal Phosphate Transport in Mice Requires Sodium-Hydrogen Exchanger Regulatory Factor-1 (NHERF-1) and Synergizes with Parathyroid Hormone. *J Biol Chem.* 2011;286(43):37216-37221.

41. Zhang MYH, Wang XM, Wang JT, et al. Dietary phosphorus transcriptionally regulates 25-hydroxyvitamin D-1 alpha-hydroxylase gene expression in the proximal renal tubule. *Endocrinology.* 2002;143(2):587-595.
42. Moolenbeek C, Ruitenberg EJ. The Swiss Roll - a Simple Technique for Histological Studies of the Rodent Intestine. *Lab Anim.* 1981;15(1):57-59.
43. Biber J, Stieger B, Stange G, Murer H. Isolation of renal proximal tubular brush-border membranes. *Nat Protoc.* 2007;2(6):1356-1359.
44. Stoll R, Kinne R, Murer H. Effect of dietary phosphate intake on phosphate transport by isolated rat renal brush-border vesicles. *Biochem J.* 1979;180(3):465-470.
45. Custer M, Lotscher M, Biber J, Murer H, Kaissling B. Expression of Na-P-I Cotransport in Rat-Kidney - Localization by Rt-Pcr and Immunohistochemistry. *Am J Physiol.* 1994;266(5):F767-F774.
46. Nowik M, Picard N, Stange G, et al. Renal phosphaturia during metabolic acidosis revisited: molecular mechanisms for decreased renal phosphate reabsorption. *Pflug Arch Eur J Phy.* 2008;457(2):539-549.
47. van der Hagen EA, Lavrijsen M, van Zeeland F, et al. Coordinated regulation of TRPV5-mediated Ca(2)(+) transport in primary distal convolution cultures. *Pflugers Arch.* 2014;466(11):2077-2087.

Figure legends

Figure 1: Expression of Pit-1/*Slc20a1*, Pit-2/*Slc20a2* and NaPi-IIb/*Slc34a3* mRNA along the intestinal tract of +/+ and f/f mice. mRNA expression of (a) Pit-1, (b) Pit-2 and (c) NaPi-IIb in samples from duodenum= D, jejunum= J, ileum= I, proximal colon= PC and distal colon= DC of wild types (+/+; n= 9) *and* Pit-2*/Slc20a2* homozygous mice (f/f; n= 5). The expression of the cotransporters was normalized to the abundance of HPRT. Data are given as mean ± SEM and statistical significances were calculated with ANOVA test. ‡ $P \leq 0.001$ and ‡‡ $P \leq 0.0001$ between the indicated segments of +/+ (a-c), or between +/+ and f/f mice for a given intestinal fragment (a, b). RNAscope analysis of (d, d1) Pit-2 and (e, e') NaPi-IIb, together with (f) positive (Ppib) and (g) negative (DapB) controls, in ileum of wild type mice. Arrow heads in the Pit-2 RNA scope indicate positive signals (red dots). The number of dots in the NaPi-IIb analysis (e, e') as well as with the positive control (f) was so high that it resulted in a general reddish color. Tissue structures: Mus= muscle, Crp= crypts, Vil= villi, Lu= lumen.

Figure 2. Protein expression of NaPi-IIb and uptakes of Pi. (a) Protein expression of NaPi-IIb (top) and β-actin (bottom) in homogenates of ileum of +/+ (n=6) and f/f mice (n= 6). Numbers on the right indicate the molecular size (kDa). (b) Uptake of ^{32}P into jejunal BBMV from +/+ (n=5) and f/f mice (n= 5). Statistical significances were calculated with ANOVA test. ‡ $P \leq 0.001$ between indicated components. (c) Paracellular fluxes of ^{32}P across samples from duodenum= D, jejunum= J, ileum= I and distal colon= DC of +/+ (n=4) and f/f mice (n=4) measured in Ussing chambers with 70 mM Pi in the apical chamber and no Pi added to the basolateral side. Statistical significances were calculated with ANOVA test. † $P \leq 0.01$ and ‡ $P \leq 0.001$ between the indicated segments of +/+ mice. All bars represent mean ± SEM.

Figure 3: Fecal, urinary and plasma concentrations of phosphate and Ca^{++} in +/+ and f/f mice fed standard or low Pi diets. The concentrations of (a-c) Pi and (d-f) Ca^{++} in (a, d) feces, (b, e) urine and (c, f) plasma were measured in samples from +/+ and f/f mice fed during the last two weeks either standard (SP) or low Pi diets (LP). The sample size is indicated by the numbers within the bars. Statistical significances were calculated with ANOVA test. ‡ $P \leq 0.001$ between diets for a given genotype; * $P \leq 0.05$ between genotypes.

Figure 4: Relative expression of Pit-1/*Slc20a1*, Pit-2/*Slc20a2* and NaPi-IIb/*Slc34a3* along the intestinal tract of +/+ and f/f mice fed standard or low Pi diet. The mRNA expression of (a) Pit-1, (b) Pit-2 and (c) NaPi-IIb was quantified in samples from duodenum= D, jejunum= J, ileum= I, proximal colon= PC and distal colon= DC. The expression of each transporter in a particular intestinal segment was simultaneously

quantified in samples from +/+ and f/f mice fed standard (SP) or low Pi diets (LP). Upon normalization to the abundance of 18S, the values obtained for SP were considered as 100%. Statistical significances were calculated with ANOVA test. * $P \leq 0.05$ and † $P \leq 0.01$ between diets. (d) Protein expression of NaPi-IIb (top) and β-actin (bottom) in homogenates of ileum of +/+ (n=6) and f/f mice fed low Pi diet (n= 5). Numbers on the right indicate the molecular size (kDa).

Figure 5: Plasma levels of phosphaturic hormones and expression renal Slc34 transporter in +/+ and f/f mice fed standard or low Pi diet. Plasma levels of (a) PTH and (b) FGF-23 were measured in samples from +/+ and f/f mice fed standard (SP) or low Pi diets (LP). The sample size is indicated by the numbers within the bars. Significances were calculated with ANOVA test. † $P < 0.01$ and ‡ $P \leq 0.001$ between diets for a given genotype. (c) Protein expression of NaPi-IIa (top), NaPi-IIc (middle) and β-tubulin (bottom) in renal homogenates. The sample size was n= 6 for all groups. Numbers on the right indicate the molecular size (kDa). Upon normalization to β-tubulin, the expression in the +/+ SP group was considered as 100%. Statistical significances were calculated with ANOVA test. † $P \leq 0.01$ and ‡ $P \leq 0.001$ between diets for a given genotype. (d) Renal mRNA expression of Pit-2. Expression of (e) Pit-2 and (f) Pit-1 mRNAs in bones. All bars represent mean ± SEM.

Figure 6: Plasma levels of $1,25(OH)_2$ vitamin D_3, renal expression of 1,25(OH)2 vitamin D_3- regulatory proteins and urinary excretion of DPD in +/+ and f/f mice fed standard or low Pi diet. (a) Plasma levels of $1,25(OH)_2$ vitamin D_3 were measured in samples from +/+ and f/f mice fed standard (SP) or low Pi diets (LP). The sample size is indicated by the numbers within the bars. Significances were calculated with ANOVA test. † $P \leq 0.01$ between diets for a given genotype and between genotypes fed on LP. mRNA expression of (b) Cyp27b1, (c) Cyp24a1 and (e) VDR was also quantified in the four experimental groups and normalized to the abundance of 18S. Statistical significances were calculated with ANOVA test. * $P \leq 0.05$ between diets for a given genotype. (d) Protein expression of Cyp24a1 (top), VDR (middle) and β-tubulin in renal homogenates. Numbers on the right indicate the molecular size (kDa). Upon normalization to β-tubulin, the expression in the +/+ SP group was considered as 100%.

Figure 7: Renal expression of Trpv5 and calbindin D28k in +/+ and f/f mice fed standard or low Pi diet. The protein expression of (a) Trpv5 and (b) calbindin D28K was quantified in renal homogenates from +/+ and f/f mice fed standard (SP) or low Pi diets (LP). Numbers on the right indicate the molecular size (kDa). Upon normalization to β-tubulin, the expression in the +/+ SP group was considered as 100%. Statistical significances were calculated with ANOVA test. (c) Urinary excretion of DPD normalized to excretion of creatinine.

Supplementary Figure 1: Generation of intestinal Pit-2/*Slc20a2* knockout mice. (a) Schematic representation of the *Slc20a2* gene (top), targeting vector (middle) and floxed allele (bottom). The gene consists of 11 exons (rectangles), with the starting codon in exon 2 and the stop codon in exon 11; both codons are indicated by asterisks. The targeting vector contained a cassette for production of β-galactosidase (β-gal) consisting of the engrailed-2 splice acceptor (En2/SA), the internal ribosome entry site (IRES), the *lacZ* gene and a polyadenylation site (pA). This cassette was followed by the phosphoglycerate kinase (PGK)-driven neomycin phosphotransferase gene (neo). This whole sequence was flanked by *FRT* sites (represented by the black ellipses), and was followed by two *loxP* sites (shaded triangles) flanking exon 4. (b) PCR screening of pups born upon blastocyst implantation into a pseudo-pregnant female: the presence of the loxed-gene in the first generation of pups upon morula aggregation and implantation was analyzed by PCR using two different combinations of primers. One combination (Slc20a2-for + loxR) is expected to produce an amplicon of 328 bp in the mutated gene, and no amplification in wild types since the antisense primer overlaps with the 3' loxP site, whereas the second combination (Slc20a2-5'arm + LAR3 + Slc20a2-3'arm) should result in 246 and 410 bp fragments in loxed and wild type DNA, respectively. Genotyping with Slc20a2-for and LoxR primers (top panel) produced the expected 328 bp amplicon in floxed mice and no amplification in wild types whereas genotyping with Slc20a2-5'arm, LAR3 and Slc20a2-3'arm (bottom panel) resulted in a 410 bp amplicon in wild type animals and a 246 bp fragment in floxed littermates. The second last and last lanes correspond to negative (no DNA) and positive (targeting plasmid: DO5) reactions. The location of PCR primers is shown below the scheme of the floxed allele. (c) Schematic representations of the conditional allele upon excision of the β-galactosidase and neo cassettes by breeding with 64FlpeB6 mice (top) as well as upon Cre-mediated excision of the floxed-sequence (bottom). (d) PCR genotyping of pups born from heterozygous floxed and Cre positive parents: amplification with the Slc20a2-5'arm and Slc20a2-3'arm primers produced amplicons of 410 bp in wild type pups (+/+) and a fragment bigger than 500 bp in homozygous floxed mice (f/f); both amplicons were generated in samples from heterozygous floxed mice (f/+).

Supplementary Figure 2: Immunostainings of jejunum with a polyclonal Pit-2 antibody. (a) Untreated and (b) 0.3% Triton-X100 treated cryosections of jejunum from +/+ mice were stained with a polyclonal antibody raised in rabbit against rat Pit-2 (red), as well as with phalloidin to detect actin (green) and DAPI to visualize nuclei (blue). As negative controls, some samples untreated (c) and triton-treated samples (d) were processed in parallel without primary antibodies.

Supplementary Figure 2 cont: Immunostainings of OK cells with a polyclonal Pit-2 antibody. (a, b) OK cells transiently transfected with a plasmid encoding for myc-fused mouse Pit-2 were stained with the

polyclonal antibody raised in rabbit against the rat cotransporter (green) together with an anti-myc monoclonal antibody raised in mouse (red) and DAPI (blue).

Supplementary Figure 3: **Immunostainings of jejunum with a monoclonal Pit-2 antibody.** 0.3% Triton-X100 treated cryosections of jejunum from (a, b) +/+ and (c, d) f/f mice were incubated with (a, c) or without (b, d) a monoclonal antibody raised against mouse Pit-2 (red), as well as with phalloidin for detection of actin (green) and DAPI to visualize nuclei (blue).

Supplementary Figure 4: Western blots of jejunal homogenates with polyclonal and monoclonal Pit-2 antibodies. Membranes containing jejunal homogenates from f/f mice fed standard diet (n=4) as well as from +/+ mice fed standard (n=5) or low phosphate diets (n=5) were incubated with (a) a polyclonal antibody raised in rabbit against rat Pit-2 or with (c) a monoclonal Pit-2 antibody raised against the mouse protein. Upon stripping, both blots were incubated with a monoclonal anti actin antibody (b, d). Molecular size markers were loaded onto the fifth wells, and sizes (kDa) are indicated on the left.

Supplementary Figure 5: **Western blots of renal homogenates with polyclonal and monoclonal Pit-2 antibodies.** Membranes containing renal homogenates from f/f mice fed standard diet (n=4) as well as from +/+ mice fed standard (n=5) or low phosphate diets (n=5) were incubated with (a) a polyclonal antibody raised in rabbit against rat Pit-2 or with (c) a monoclonal Pit-2 antibody raised against the mouse protein. Upon stripping, both blots were incubated with a monoclonal anti actin antibody (b, d). Molecular size markers were loaded onto the fifth wells, and sizes (kDa) are indicated on the left.

Supplementary Figure 6: Intestinal basolateral recovery of ^{32}P is linear within 2 hours time-course. Recovery of ^{32}P from the basolateral side upon incubating samples from duodenum, jejunum, ileum and distal colon of +/+ mice in Ussing chambers with a 70 mM apical-to-basolateral gradient of Pi. Basolateral aliquots were sampled just before addition of ^{32}P as well as 60, 90 and 120 minutes after apical administration of the tracer. Data are presented as mean ± SEM for 4 independent experiments

Supplementary Figure 7: Expression of Pit-1/*Slc20a1*, Pit-2/*Slc20a2* and NaPi-IIb/*Slc34a3* along the intestinal tract of +/+ and f/f mice fed standard or low Pi diet. The mRNA expression of (top graphs) Pit-1, (middle graphs) Pit-2 and (bottom graphs) NaPi-IIb was quantified by real time PCR in samples from duodenum= D, jejunum= J, ileum= I, proximal colon= PC and distal colon= DC. The expression of each transporter in a particular intestinal segment was simultaneously quantified in samples from +/+ and f/f mice fed standard (SD) or low Pi diets (LP) and the expression was normalized to the abundance of 18S. Statistical significances were calculated with ANOVA test. * $P< 0.05$, † $P \leq 0.01$ and ‡ $P \leq 0.001$ between the indicated groups

Table 1: Sequences of primers and probes used for genotyping and real time PCR.

Table 1

Oligo	Sequence
Slc20a2-for	CCACTTCTTTCTGGCTTCATGTCC
Slc20a2-5'arm	TAGATATGGAGGAATGAGAGCAGC
Slc20a2-3'arm	CCATGCGTCAGAGCTCAGGAATCC
LoxR	TGAACTGATGGCGAGCTCAGACC
LAR3	CAACGGGTTCTTCTGTTAGTCC
CRE3	TCGCTGCATTACCGGTCGATGC
CRE4	CCATGAGTGAACGAACCTGGTCG
Pit-1/Fw	CGCTGCTTTCTGGTATTATGTCTG
Pit-1/Rv	AGAGGTTGATTCCGATTGTGCA
Pit-1/Pb	TTGTTCGTGCGTTCATCCTCCGTAAGG
Pit-2/Fw	AGGAGTGCAGTGGATGGAGC
Pit-2/Rv	ATTAGTATGAACAGCACGCCGG
Pit-2/Pb	ATTGTCGCCTCCTGGTTTATATCGCCAC
NaPi-IIb/Fw	CTTGGGACCTGCCTGAAC
NaPi-IIb/Rv	AATGCAGAGCGTCTTCCCTTT
NaPi-IIb/Pb	TGGTCAGAGAGAGACAC

Fig 1

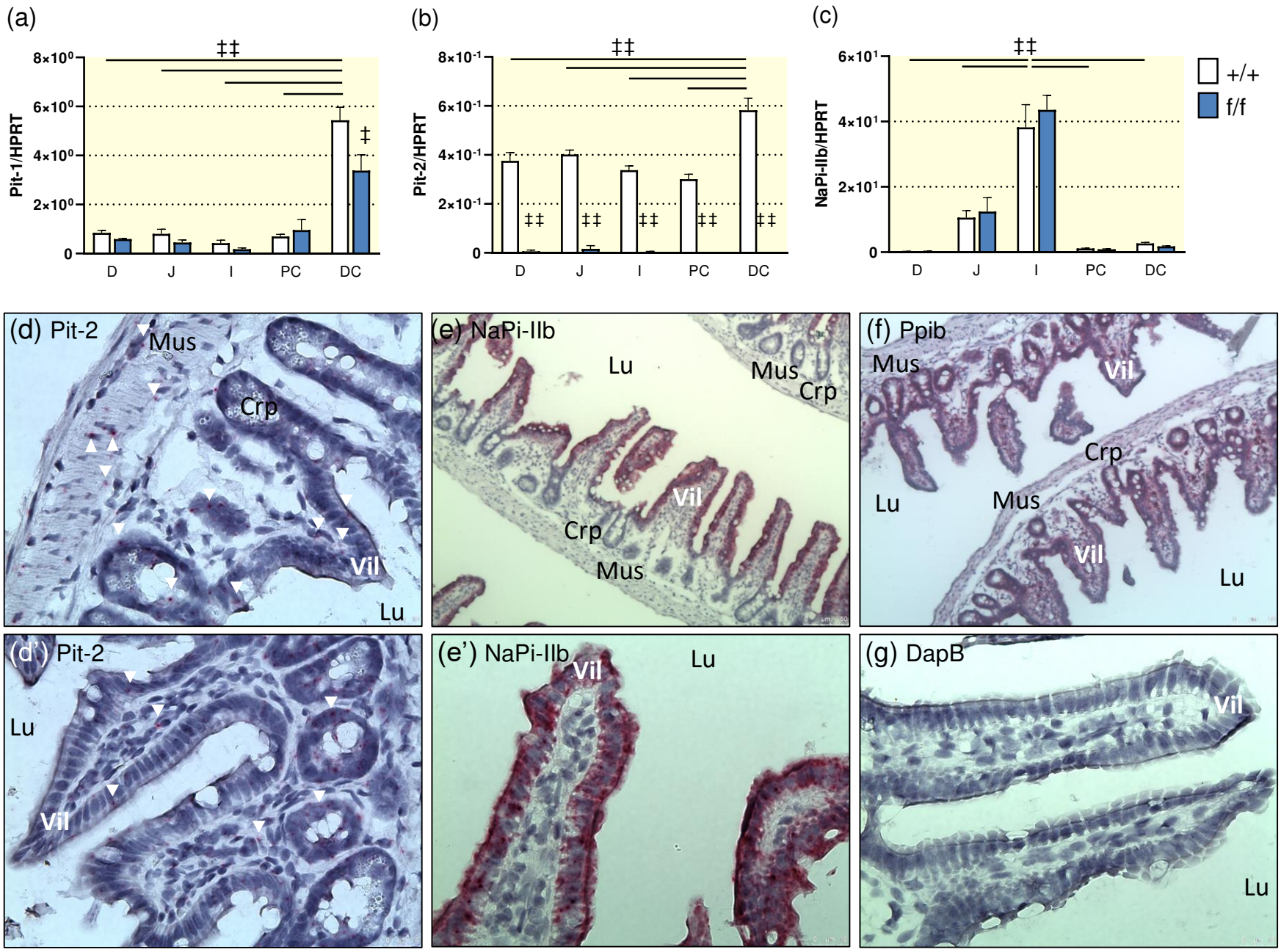
(a)
Pit-1/HPRT
8×10⁰
6×10⁰
4×10⁰
2×10⁰
0
D
J
I
PC
DC
‡‡
‡
(b)
Pit-2/HPRT
8×10⁻¹
6×10⁻¹
4×10⁻¹
2×10⁻¹
0
‡‡
(c)
NaPi-IIb/HPRT
6×10¹
4×10¹
2×10¹
+/+
f/f
(d) Pit-2
Mus
Crp
Vil
Lu
(e) NaPi-IIb
Lu
Mus
Crp
Vil
(f) Ppib
Mus
Vil
Crp
Lu
(d') Pit-2
(e') NaPi-IIb
(g) DapB

Fig 2

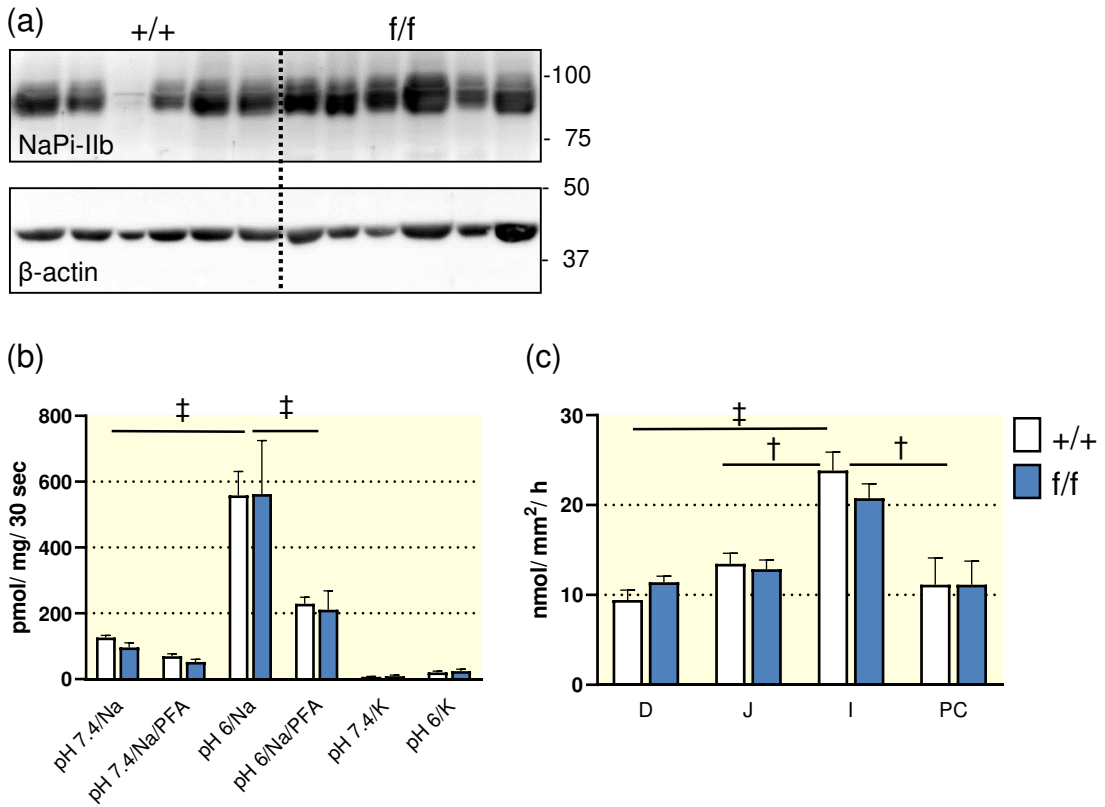
(a)
+/+
f/f
100
75
50
37
NaPi-IIb
β-actin
(b)
pmol/ mg/ 30 sec
800
600
400
200
0
‡
‡
pH 7.4/Na
pH 7.4/Na/PFA
pH 6/Na
pH 6/Na/PFA
pH 7.4/K
pH 6/K
(c)
nmol/ mm2/ h
30
20
10
0
‡
†
†
D
J
I
PC
+/+
f/f

Fig 3

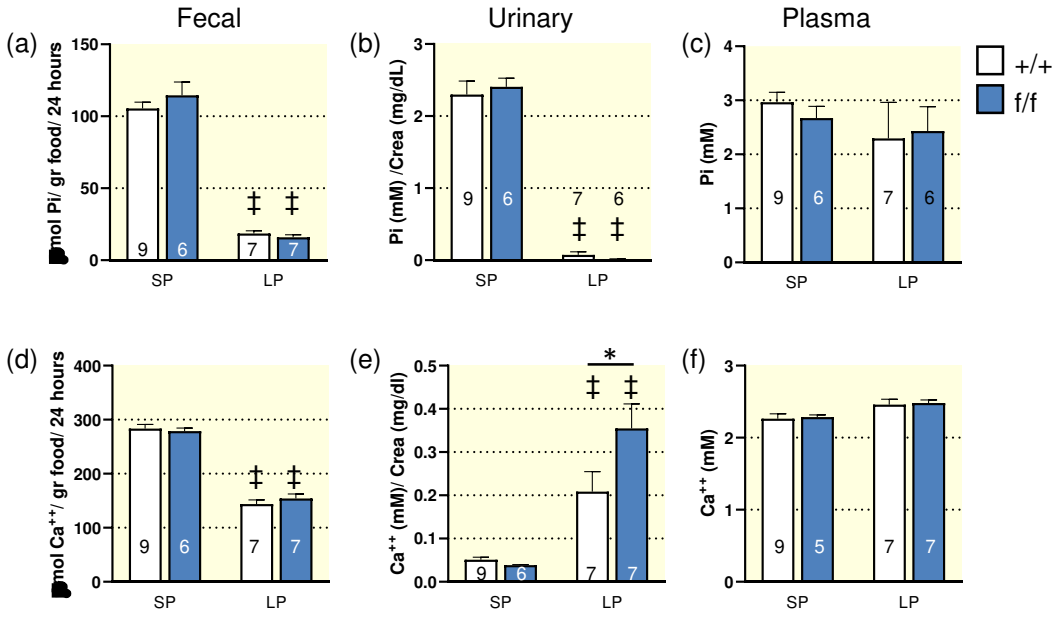
Fecal
Urinary
Plasma
(a)
(b)
(c)
(d)
(e)
(f)
+/+
f/f
mol Pi/ gr food/ 24 hours
Pi (mM) /Crea (mg/dL)
Pi (mM)
mol Ca++/ gr food/ 24 hours
Ca++ (mM)/ Crea (mg/dl)
Ca++ (mM)
SP
LP
9
6
7
5
‡
*

Fig 4

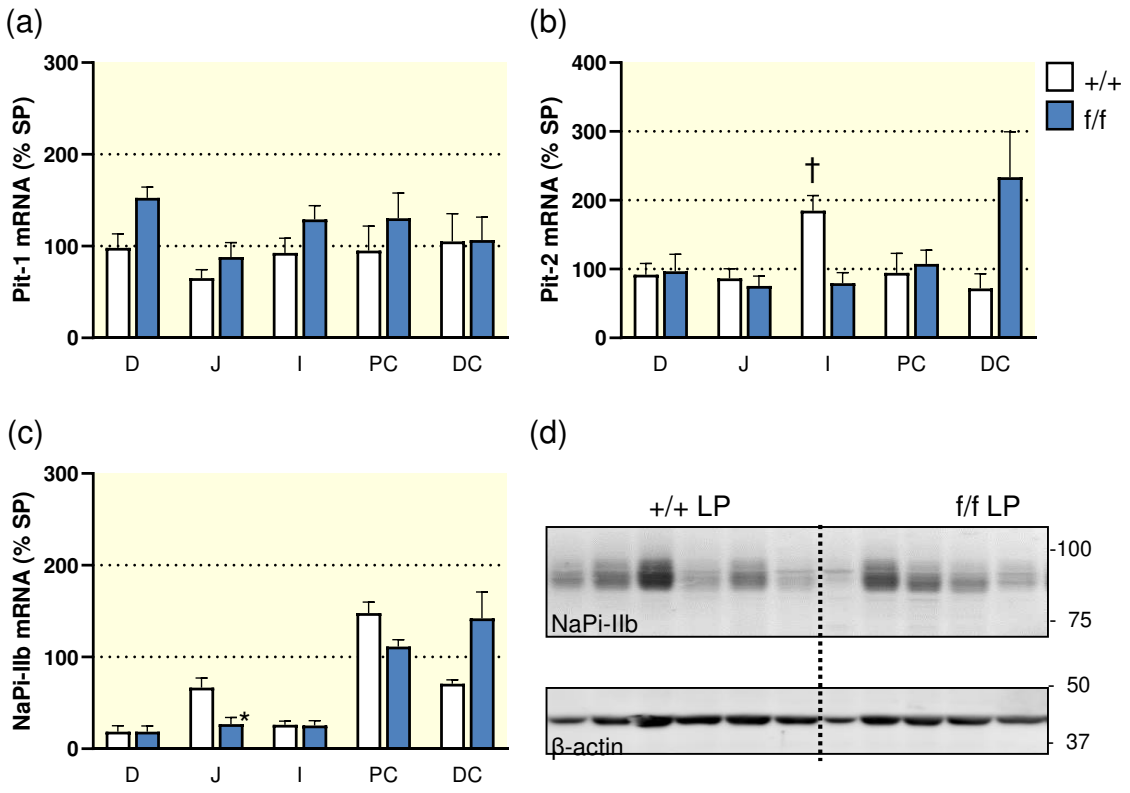
(a)
Pit-1 mRNA (% SP)
300
200
100
0
D
J
I
PC
DC
(b)
Pit-2 mRNA (% SP)
400
300
200
100
0
†
+/+
f/f
(c)
NaPi-IIb mRNA (% SP)
*
(d)
+/+ LP
f/f LP
NaPi-IIb
β-actin
100
75
50
37

Fig 5

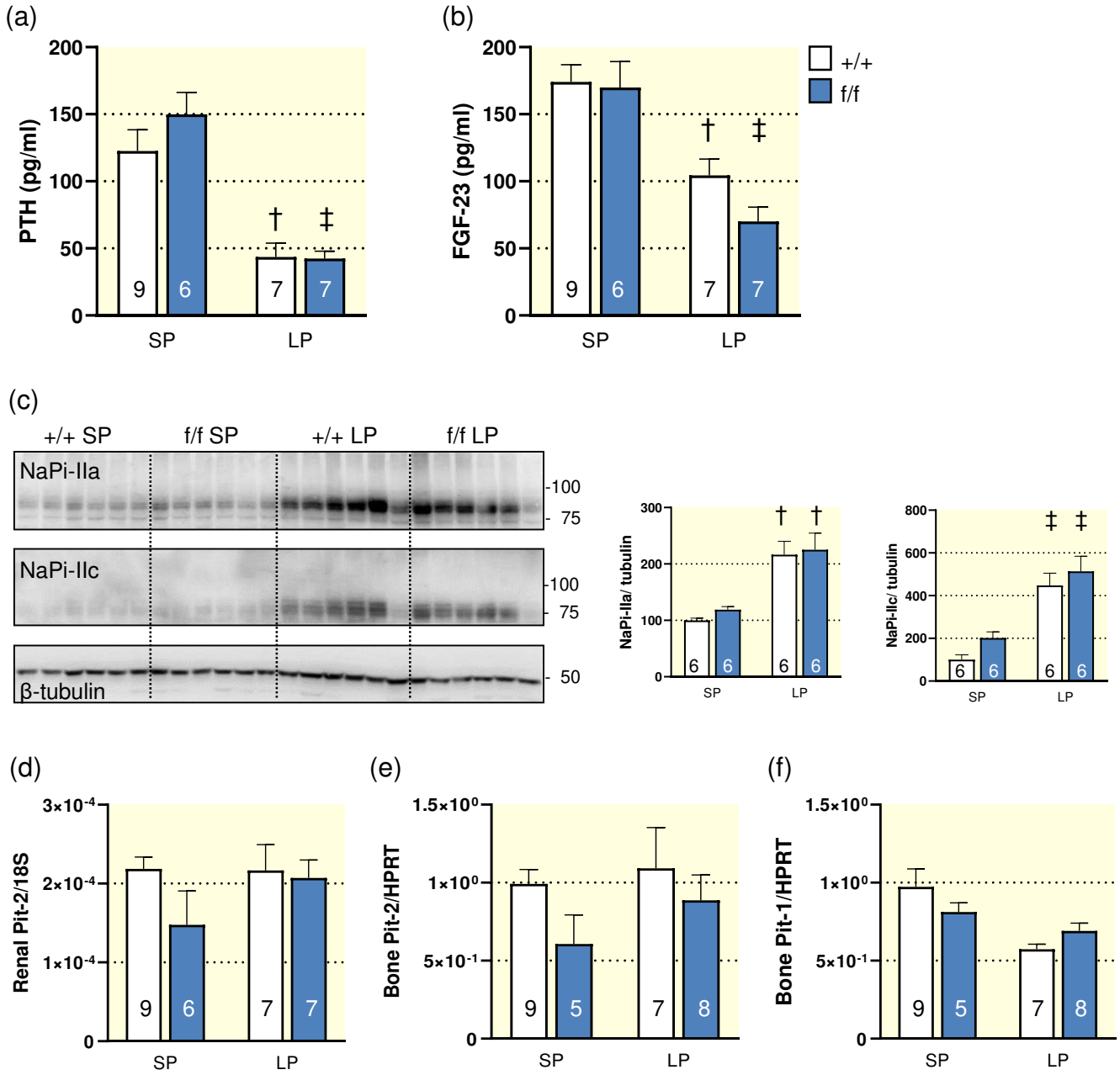
(a)
PTH (pg/ml)
200
150
100
50
0
9
6
7
7
†
‡
SP
LP
(b)
FGF-23 (pg/ml)
+/+
f/f
(c)
+/+ SP
f/f SP
+/+ LP
f/f LP
NaPi-IIa
NaPi-IIc
β-tubulin
100
75
50
NaPi-IIa/ tubulin
NaPi-IIc/ tubulin
(d)
Renal Pit-2/18S
3×10-4
2×10-4
1×10-4
(e)
Bone Pit-2/HPRT
1.5×100
1×100
5×10-1
5
8
(f)
Bone Pit-1/HPRT

Fig 6

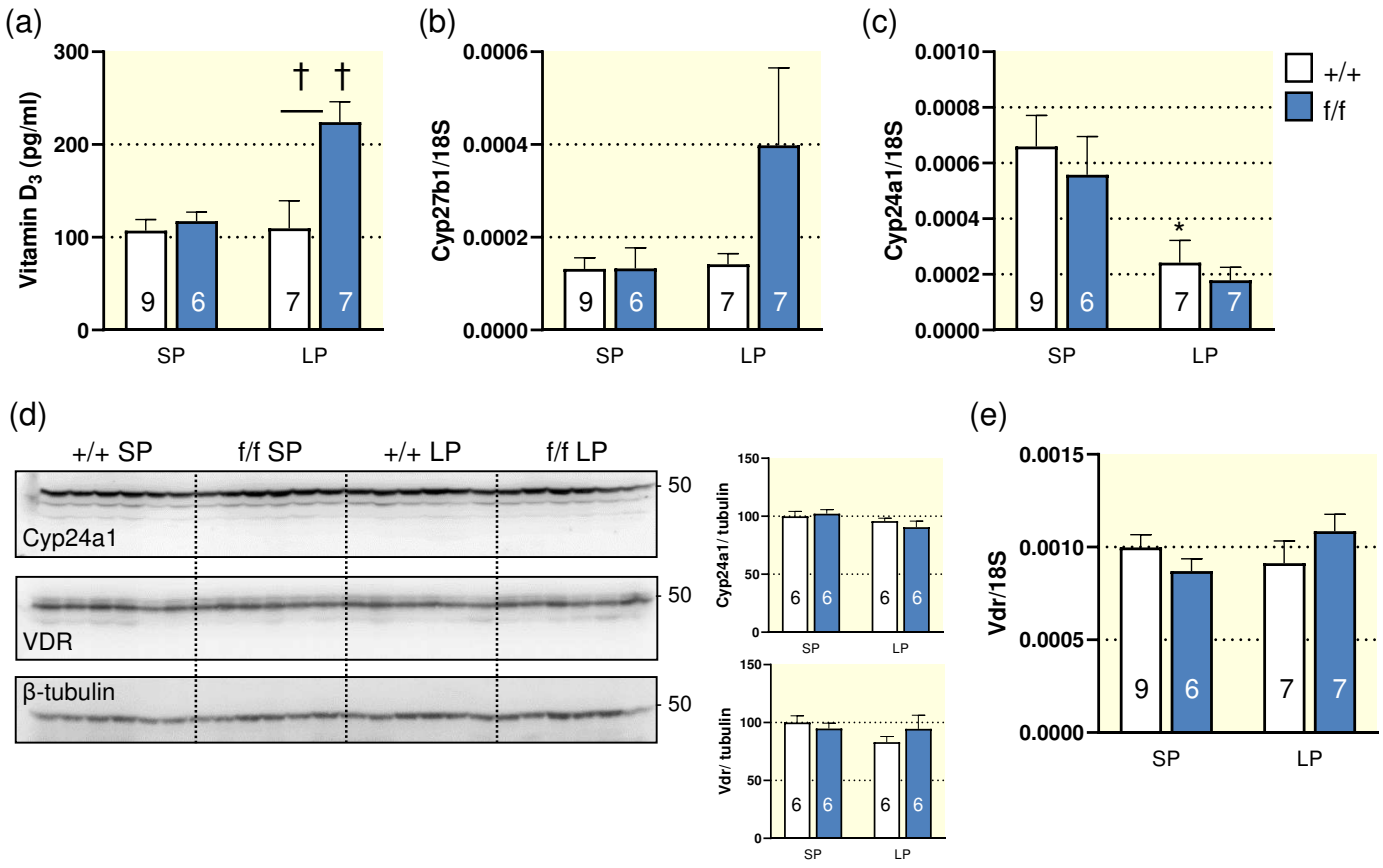
(a)
Vitamin D3 (pg/ml)
300
200
100
0
†
†
9
6
7
7
SP
LP
(b)
Cyp27b1/18S
0.0006
0.0004
0.0002
0.0000
9
6
7
7
SP
LP
(c)
Cyp24a1/18S
0.0010
0.0008
0.0006
0.0004
0.0002
0.0000
*
+/+
f/f
9
6
7
7
SP
LP
(d)
+/+ SP
f/f SP
+/+ LP
f/f LP
Cyp24a1
VDR
β-tubulin
50
50
50
Cyp24a1/ tubulin
150
100
50
0
6
6
6
6
SP
LP
Vdr/ tubulin
150
100
50
0
6
6
6
6
SP
LP
(e)
Vdr/18S
0.0015
0.0010
0.0005
0.0000
9
6
7
7
SP
LP

Fig 7

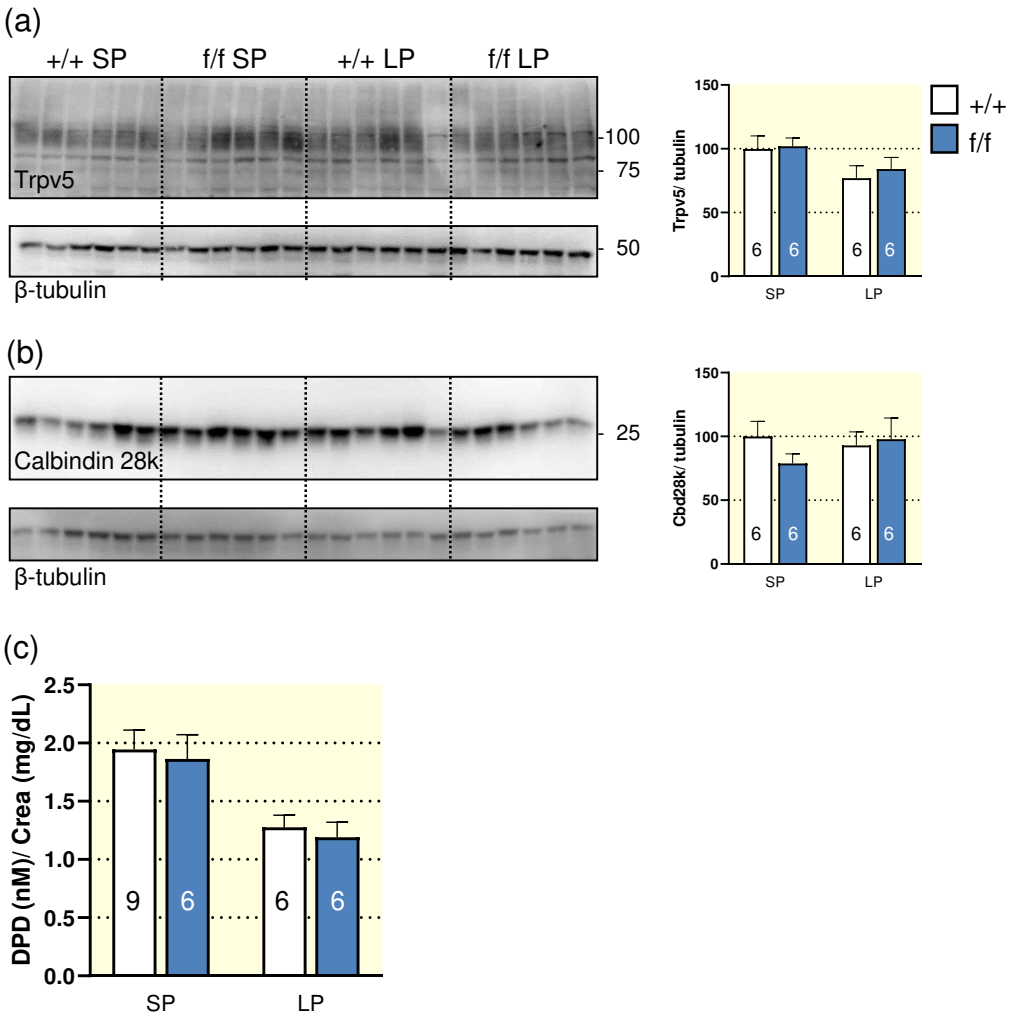
(a)
+/+ SP
f/f SP
+/+ LP
f/f LP
Trpv5
100
75
50
β-tubulin
Trpv5/ tubulin
+/+
f/f
(b)
Calbindin 28k
25
β-tubulin
Cbd28k/ tubulin
(c)
DPD (nM)/ Crea (mg/dL)
SP
LP